

Tunable transport bandgap in narrow bilayer graphene nanoribbons

Woo Jong Yu¹ and Xiangfeng Duan^{1,2,*}

¹Department of Chemistry and Biochemistry, University of California, Los Angeles, CA 90095, USA; ²California Nanosystems Institute, University of California, Los Angeles, CA 90095, USA

Supplementary Information

1. Classification of monolayer and bilayer graphene.
2. Characteristics of Si/Al₂O₃ core/shell nanowire.
3. Optical images of the fabrication procedures of dual-gated bilayer graphene nanoribbon FET.
4. Transfer characteristics of a bilayer GNR FET at various temperatures.
5. Switching behavior of monolayer GNR FET.

1. Classification of monolayer and bilayer graphene.

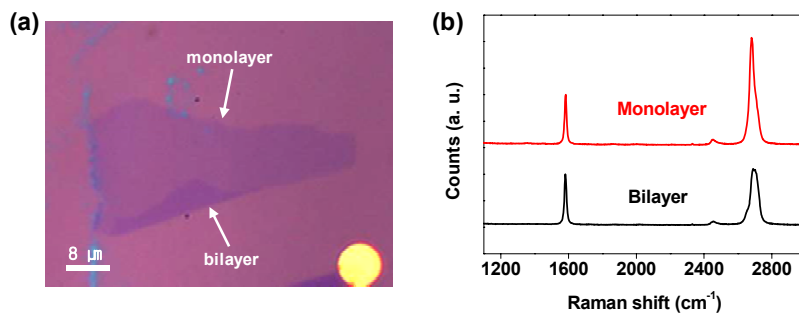


Figure S1. a, Optical microscopy image of exfoliated monolayer and bilayer graphene. b, Raman spectra of exfoliated monlayer (red line, top), and bilayer graphene (black line, bottom). Laser excitation wavelength of 514 nm was used.

2. Characteristics of Si/Al₂O₃ core/shell nanowires.

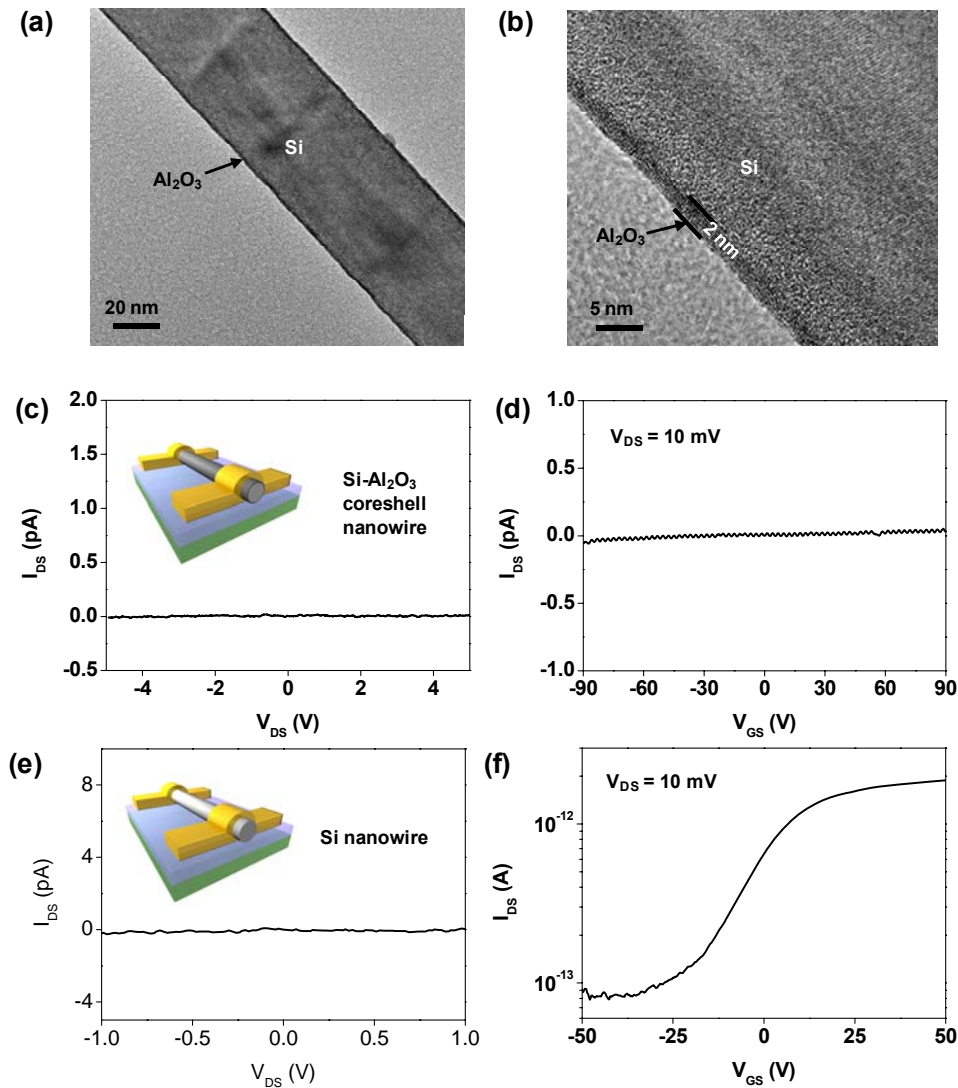


Figure S2. **a**, TEM and **b**, HRTEM images of an Si/Al₂O₃ core/shell nanowire. 2 nm Al₂O₃ is uniformly coated on the Si nanowire surface by ALD to prevent current flow through the Si nanowire. **c**, I_{DS} - V_{DS} characteristics of an Si/Al₂O₃ core/shell nanowire. The inset is the schematic image of Si/Al₂O₃ core/shell nanowire devices. **d**, Transfer characteristics of Si/Al₂O₃ core/shell nanowire at $V_{DS} = 10$ mV. Si/Al₂O₃ core/shell nanowire has negligible current because of the Al₂O₃ dielectric layer and undoped Si nanowires. **e**, I_{DS} - V_{DS} characteristics of an undoped Si nanowire. Inset is the schematic image of Si nanowire devices. **f**, Transfer characteristics of the undoped Si nanowire at $V_{DS} = 10$ mV.

3. Optical images of the fabrication procedure of dual-gated bilayer graphene nanoribbon FET.

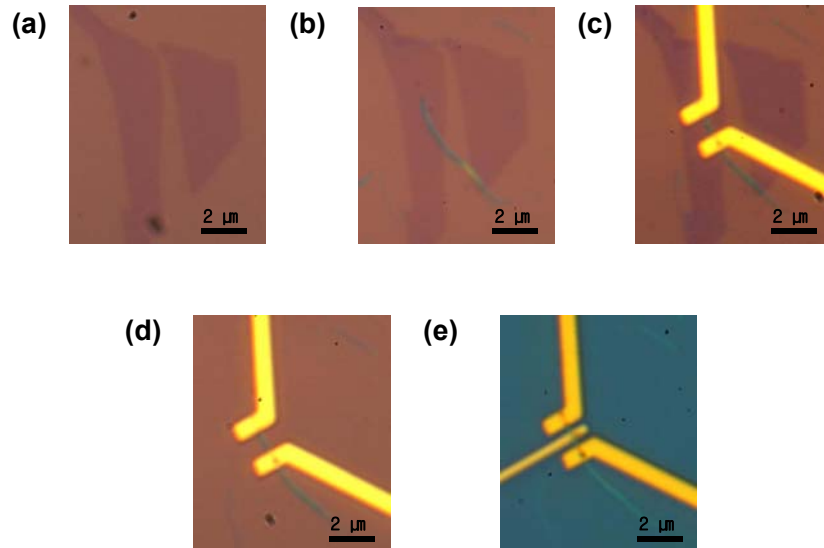


Figure S3. **a**, Two pieces of mechanically exfoliated bilayer graphene on the Si wafer with 300 nm SiO₂. **b**, Si/Al₂O₃ core/shell nanowire was transferred onto bilayer graphene. **c**, Source and drain electrodes were formed on aligned bilayer graphene and Si/Al₂O₃ core/shell nanowire. **d**, Uncovered bilayer graphene was etched by oxygen plasma, and bilayer graphene nanoribbon was produced under the Si nanowire. **e**, A 60-nm HfO₂ thin film and top gate electrode was deposited in the final step.

4. Transfer characteristics of a bilayer GNR FET at various temperatures.

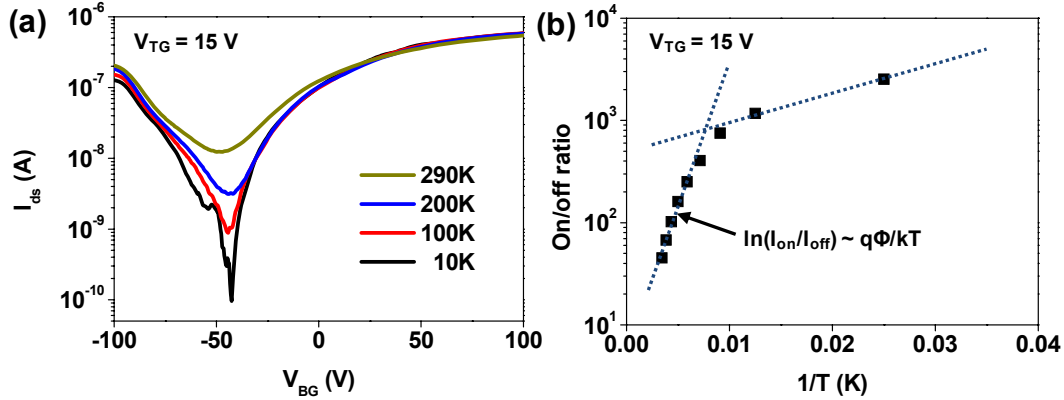


Figure S4. a, Temperature dependent transfer characteristics of bilayer GNR FET at $V_{TG} = 15$ V. **b**, The device on/off current ratio vs. temperature at $V_{TG} = 15$ V. The dash line at high temperature region is a fit to simple thermal activated transport, and the dash line at low temperature region is a fit to quasi-1D variable range hopping¹. The off current (I_{off}) for thermionic injection is proportional to $\exp(-q\phi_{barrier}/k_B T)$ above about 100K, thus $\ln(I_{on}/I_{off})$ vs $1/T$ plot would yield a straight line with a slope of $q\phi_{barrier}/k_B$ ^{2,3}. The dashed line denotes the estimated on/off ratio vs temperature for a transport gap of 181 meV, which is comparable with transport gap of 197 meV obtained from

$$I_{on}/I_{off} \approx \exp(-q\phi_{barrier}/k_B T) \text{ at } 290\text{K. Moreover, the on/off current ratio does not}$$

improve as fast as indicated by the dashed line at temperatures below about 100 K, most likely due to the presence of tunneling through defect states, i.e., tails in the density of states^{3,4}. This phenomenon has been observed in both graphene nanoribbon^{2,3} and carbon nanotube⁴ transistors.

5. Switching behavior of monolayer GNR FET.

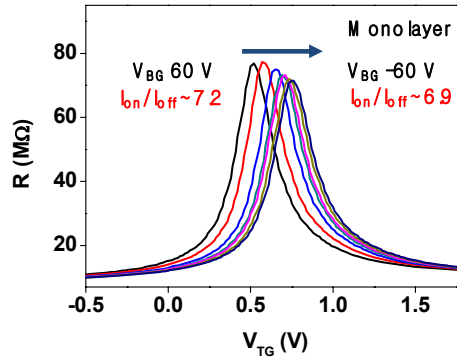


Figure S5. Switching behavior of monolayer GNR FET was measured as V_{BG} was varied from 60 V to -60 V in steps of 20 V. The on/off ratio was not significantly changed.

References

1. Bai, J. *et al.* Very large magnetoresistance in graphene nanoribbons. *Nature Nanotechnol.* **5**, 655-659 (2010).
2. Xia, F., Farmer, D. B., Lin, Y. & Avouris, Ph. Graphene field-effect transistors with high on/off current ratio and large transport bandgap at room temperature. *Nano Lett.* **10**, 715-718 (2010).
3. Chen, Z., Lin, Y. M., Rooks, M. J. & Avouris, Ph Graphene nano-ribbon electronics. *Physica E* **40**, 228 (2007).
4. Appenzeller, J., Radosavljevic, M., Knoch, J. & Avouris, Ph Tunneling versus thermionic emission in one-dimensional semiconductors. *Phys. Rev. Lett.* **92**, No. 048301 (2004).